ELSEVIER

Journal of Molecular Catalysis A: Chemical 178 (2002) 97–104

JOURNAL OF MOLECULAR CATALYSIS A: CHEMICAL

www.elsevier.com/locate/molcata

Nanosized anatase TiO_2 as precursor for preparation of sulfated titania catalysts

Zhen Ma, Yinghong Yue, Xingyi Deng, Zi Gao*

Department of Chemistry, Fudan University, Shanghai 200433, PR China

Received 14 March 2001; accepted 22 June 2001

Abstract

Nanosized anatase TiO_2 has been prepared by a sol–gel hydrothermal process. The effect of water:alkoxide molar ratio, hydrothermal aging temperature and aging time on the properties of the nanocrystalline anatase TiO_2 was investigated in detail. The specific surface area, sulfur content and surface acidity of sulfated titania catalysts prepared by sulfation of sol–gel hydrothermal derived nanocrystalline TiO_2 were greater than those of the analogous catalyst prepared from ordinary amorphous titania hydrate. The former catalysts displayed higher catalytic activities in isopropanol dehydration, cumene cracking and *n*-pentane conversion reactions. The influence of the crystalline state and crystalline grain of titania precursors on the properties of sulfated titania catalysts was studied and discussed.

Keywords: Sol–gel hydrothermal process; Nanosized TiO_2; Sulfated titania; Solid acid catalyst

1. Introduction

Sulfated metal oxides such as sulfated zirconia, titania, tin oxide and iron oxide are solid strong acids that have arisen increasing interest in recent years because of their high thermostability, strong acidity and unique catalytic activities in many environmentally benign reactions [1–5]. The method of preparation significantly affects the catalytic properties of these materials. Numerous methods have been reported in the literature in particular for the preparation of sulfated zirconia. They differ mainly in the type of oxide precursor, type of sulfating agent, method of impregnation and calcination temperature. Sometimes the results are controversial because different experimental techniques or test reactions have been used to characterize these materials. It has been reported in the literature [1,6–10] that amorphous $Zr(OH)_4$ or $Ti(OH)_4$ should be used as the precursor for sulfation to ensure high sulfur content and strong acidity, but a few authors have found that sulfated zirconia catalysts obtained by H_2SO_4 impregnation of a crystalline ZrO_2 [11] or a zirconia aerogel [12] followed by calcination have identical acidity and activity as catalysts prepared from amorphous zirconia hydrate.

Among the sulfated metal oxides, sulfated zirconia is known to possess the strongest acidity and exhibit superior activity to many acid-catalyzed reactions. Hence, a great deal of research works in this area have been concentrated on the study of this type of material. In comparison to the voluminous literatures on sulfated zirconia, knowledge of sulfated titania is limited. However, the latter material has been found to be efficient for catalyzing isomerization [13–15], alkylation [8,16–18], Friedel–Crafts acylation [19,20], esterification [21–23], CFC decomposition [24,25],

* Corresponding author. Tel.: +86-21-65642792; fax: +86-21-65641740.
E-mail address: zigao@fudan.edu.cn (Z. Gao).

1381-1169/02/$ – see front matter
PII: S1381-1169(01)00280-1

photocatalytic oxidation [26,27] and selective catalytic reduction of NO_x [28]. The increasing application of sulfated titania draws our attention to the study of the influence of preparation parameters on its properties and catalytic activities.

In this work, nanosized anatase TiO_2 was prepared by a sol–gel hydrothermal method [29] and used as the precursor for preparation of SO_4^{2-}/TiO_2. The physicochemical properties, surface acidity and catalytic activities of SO_4^{2-}/TiO_2 prepared from this type of nanosized anatase TiO_2 and conventional amorphous titania hydrate were investigated and compared in detail.

2. Experimental

2.1. Sample preparation

Anatase TiO_2 nanocrystals were prepared by a combination of conventional sol–gel hydrolysis precipitation and hydrothermal processing [29]. In a typical synthesis, 0.1 mol titanium butoxide ($Ti(OC_4H_9)_4$) was dissolved in 1.5 mol anhydrous ethanol, and the butoxide solution was added dropwise to a water–ethanol solution containing 1 mol ethanol with rigorous stirring at room temperature. The water:alkoxide molar ratio ranged between 5 and 150 in this paper. A white precipitate of hydrous oxide was formed and the mixture was stirred for 3 h. Then the mother liquor containing the amorphous precipitate was transferred to a stainless steel autoclave and aged at 80–180 °C for 1–5 days, followed by filtering, washing with deionized water and drying at 110 °C overnight. The products were denoted as SGH-TiO_2–*r*–*t*–*d*, where *r* means the water:alkoxide molar ratio, *t* the hydrothermal treatment temperature (°C) and *d* the aging time (days).

For comparison, two other precursors were prepared: (1) amorphous $Ti(OH)_4$ (A-TiO_2) was prepared by dropping aqueous ammonia to $TiCl_4$ dissolved in HCl till pH = 9–10, aging at room temperature for 24 h, washing, filtering and drying at 110 °C overnight; (2) precrystallized TiO_2 (A-TiO_2 (500 °C)) was prepared by calcining the amorphous $Ti(OH)_4$ powder at 500 °C for 3 h.

Sulfated titania samples were prepared by immersing the above titania precursors in 1 mol/l H_2SO_4 solution for 30 min, followed by filtering, drying at 110 °C overnight and calcining at 500 °C for 3 h.

2.2. Characterization

BET surface area of the samples was measured on a Micromeritics ASAP 2000 equipment using N_2 as the adsorbent. X-ray powder diffraction measurements were performed on a computer-controlled Rigaku D/MAX-IIA instrument with Cu Kα radiation at 40 kV and 20 mA with scan speed 8°/min and scan range 10–80°. The crystallite size of various samples was estimated by applying Scherrer formula on the (1 0 1) diffraction peaks of anatase TiO_2. The amount of acid sites was measured by NH_3-TPD in a flow-type fixed-bed reactor at ambient pressure. The 0.1 g sample was heated at 500 °C for 2 h and cooled to 120 °C in flowing He. At 120 °C, the sample was treated by sufficient pulses of NH_3 till adsorption saturation, followed by a He purge for about 2 h. The temperature was raised up from 120 to 500 °C at a rate of 10 °C/min to desorb NH_3, and then was further maintained at 500 °C for 0.5 h. Sulfur content of the samples was determined by a chemical method. Dehydrated Na_2CO_3 and ZnO (1:4) were used as fusing agents, and the sulfate was turned into $BaSO_4$ and detected by gravimetric method.

2.3. Reaction testing

The dehydration of isopropanol was performed in a pulsed microreactor with a catalyst load of 50 mg. The catalyst was preheated in H_2 flow at 250 °C for 3 h. H_2 was used as the carrier gas at a flow rate of 30 ml/min. The amount of isopropanol injected for each test was 5 μl and the reaction temperatures were 150, 175 and 200 °C.

The activity of the samples toward cumene cracking reaction was tested in a pulsed microreactor loaded with 50 mg catalyst. The catalyst was preheated under N_2 atmosphere at 350 °C for 3 h. H_2 was used as the carrier gas at a flow rate of 40 ml/min. The amount of cumene injected for each test was 1 μl and the reaction temperature was 300 °C.

n-Pentane conversion reaction was carried out in a pulsed microreactor under ambient pressure on 0.4 g catalyst. The catalyst was preheated under N_2 atmosphere at 400 °C for 3 h. Upon reaction, the carrier gas

was N_2 with a flow rate of 30 ml/min. The amount of *n*-pentane injected for each pulse was 0.5 μl and the reaction temperatures were 325 and 350 °C.

3. Results

3.1. Sol–gel hydrothermal derived TiO_2

In the preparation of sulfated titania, sulfation of the oxide precursor is usually carried out by immersing dried oxide precursor into a dilute H_2SO_4 solution allowing adequate adsorption of SO_4^{2-} onto the precursor. Then the sulfated precursor is calcined at a high temperature to produce highly covalent sulfate structure on the surface, which is considered as the source of the strong acidity on this type of material. It was expected that the specific surface area of the oxide precursor might exert a significant influence on the properties of the final catalyst. Thus, the effect of water:alkoxide molar ratio, aging temperature and aging time on BET surface area of sol–gel hydrothermal derived TiO_2 was investigated in detail and the results were illustrated in Fig. 1.

The BET surface area of the SGH-TiO_2 samples was sensitive to the water:alkoxide molar ratio as the water:alkoxide ratio was below 30. For most of the samples increasing the water:alkoxide ratio from 5 to 30 led to an increase in the surface area. Samples SGH-TiO_2–5–80–1, SGH-TiO_2–5–80–3, SGH-TiO_2–15–80–1 and SGH-TiO_2–15–80–3 were exceptional, because crystallization was incomplete after aging at 80 °C for 1 and 3 days. For systems with the water:alkoxide ratio greater than 30, increasing the water:alkoxide ratio had no significant effect on the BET surface area of the samples. The above observations are consistent with the results in the literature [29].

The BET surface area of SGH-TiO_2 decreased as the aging temperature was raised from 80 to 180 °C and the aging time was prolonged from 1 to 5 days. However, the effect of aging time was less pronounced than that of aging temperature. BET surface areas of the SGH-TiO_2 samples prepared with a water:alkoxide ratio of 50 were in the range of 149–223 m^2/g. The calculated equivalent sizes of TiO_2 nanocrystals would be 6.9–10.3 nm, assuming a monodispersed spherical morphology.

The variation of BET surface area with calcination temperature for various titania samples was illustrated in Fig. 2. The surface area of A-TiO_2 decreased drastically at 300–350 °C when the phase transformation from amorphous titania to anatase was accomplished. Although the initial surface areas of SGH-TiO_2 samples were smaller than that of A-TiO_2, the reduction in their surface area with calcination temperature was much slower, showing that nanocrystals of anatase TiO_2 prepared by sol–gel hydrothermal process are thermally more stable than amorphous TiO_2. At calcination temperatures above 350 °C, BET surface areas of the samples were in the order of A-TiO_2 < SGH-TiO_2–

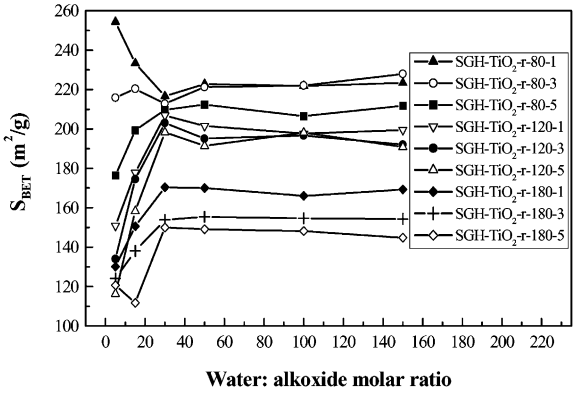

Fig. 1. Effect of preparation parameters (water:alkoxide ratio, hydrothermal aging temperature and aging time) on BET surface area of sol–gel hydrothermal derived TiO_2.

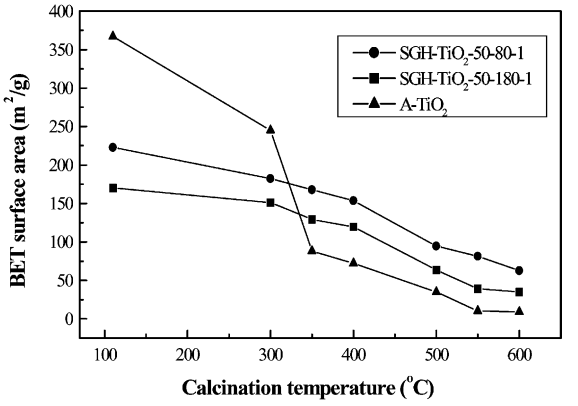

Fig. 2. Variation of BET surface area with calcination temperature for various TiO_2 samples.

Table 1
Physicochemical properties of various precursors and catalysts

Samples	S_{BET} (m^2/g)	Total pore volume (cm^3/g)	Average pore size (nm)	Crystallite size (nm)	SO_3 (wt.%)	NH_3-TPD acidity (mmol/g)
A-TiO_2	367	0.26	2.9	–	–	–
A-TiO_2(500 °C)	34.8	0.06	7.3	50	–	0.23
SGH-TiO_2–50–180–1	169	0.28	6.7	10	–	–
SGH-TiO_2–50–80–1	223	0.29	5.3	6.5	–	–
SGH-TiO_2–50–180–1 (500 °C)	62.9	0.14	8.9	25	–	–
SGH-TiO_2–50–80–1 (500 °C)	94.5	0.20	8.7	15	–	–
SO_4^{2-}/A-TiO_2	101	0.12	4.6	12	3.3	0.66
SO_4^{2-}/A-TiO_2 (500 °C)	24.8	0.06	8.9	65	0.6	0.45
SO_4^{2-}/SGH-TiO_2–50–180–1	120	0.28	9.4	12	3.2	0.72
SO_4^{2-}/SGH-TiO_2–50–80–1	138	0.23	6.8	10	3.6	0.79

50–180–1 < SGH-TiO_2–50–80–1. For example, BET surface areas of A-TiO_2, SGH-TiO_2–50–180–1 and SGH-TiO_2–50–80–1 calcined at 500 °C were 34.8, 62.9 and 94.5 m^2/g, respectively (see Table 1).

XRD patterns of SGH-TiO_2 samples prepared with a water:alkoxide ratio of 50 were compared with those of A-TiO_2 and A- TiO_2 (500 °C) in Fig. 3. A-TiO_2 prepared by hydrolysis of $TiCl_4$ with ammonia solution was amorphous in nature and had a high BET surface area of 367 m^2/g. A-TiO_2 (500 °C) obtained by calcining A-TiO_2 at 500 °C was crystalline anatase with intense diffraction peaks, as its BET surface area was only 34.8 m^2/g. All the SGH-TiO_2 samples displayed low and broad diffraction peaks of anatase TiO_2. The crystallite sizes of the SGH-TiO_2 samples aged at 80, 120 and 180 °C for 1 day were estimated to be 6.5, 7.5 and 10 nm, respectively, by applying Scherrer formula on the (1 0 1) diffraction peaks. These results coincide very well with those calculated from BET surface areas.

XRD patterns of various TiO_2 samples calcined at 500 °C were compared in Fig. 4. No rutile peaks were detected in all these patterns. The intensity of the anatase peaks decreased in the order of A-TiO_2 (500 °C) > SGH-TiO_2–50–180–1 > SGH-TiO_2–50–80–1, and the estimated crystallite sizes of those three samples using Scherrer formula were 50, 25 and 15 nm, respectively. This further confirms that the nanocrystals of SGH-TiO_2 are thermally more stable. After calcination at 500 °C, the crystallite sizes of SGH-TiO_2 are two-fold or three-fold smaller than that of A-TiO_2 (500 °C).

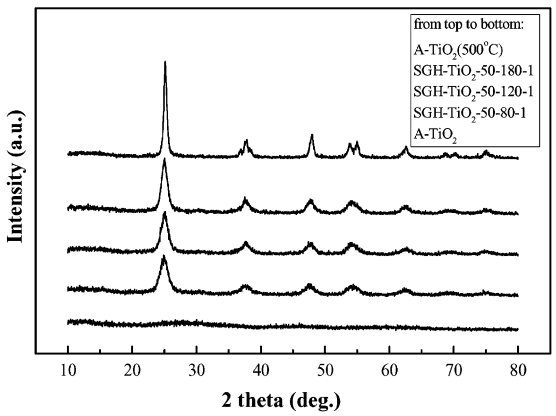

Fig. 3. XRD patterns of TiO_2 samples prepared in different ways.

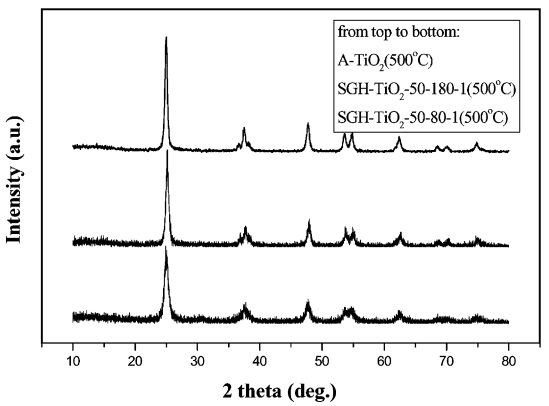

Fig. 4. XRD patterns of various TiO_2 samples calcined at 500 °C.

3.2. Sulfated titania catalysts

Sulfated titania catalysts were prepared using A-TiO_2, A-TiO_2 (500 °C), SGH-TiO_2–50–180–1 and SGH-TiO_2–50–80–1 as precursors and characterized. The characterization results of the catalysts were listed and compared with those of the neat precursors in Table 1.

BET surface areas of SO_4^{2-}/A-TiO_2, SO_4^{2-}/SGH-TiO_2–50–180–1 and SO_4^{2-}/SGH-TiO_2–50–80–1 calcined at 500 °C were lower than those of the non-calcined precursors but higher than those of the precursors calcined at 500 °C. The XRD characteristic peaks of anatase TiO_2 for these SO_4^{2-}/TiO_2 samples calcined at 500 °C were lower and broader than those for the corresponding precursors calcined at 500 °C, as shown in Fig. 5. These observations are in support of the generally recognized viewpoint that sulfation inhibits the sintering of titania and stabilizes the surface area of sulfated titania catalyst [4]. Data in Table 1 show that finer anatase crystallites are found in sulfated titania catalysts than in pure titania calcined at the same temperature, which accounts for the smaller reduction in surface area upon calcination for the sulfated titania catalysts. The measured BET surface areas of the catalysts were in the order of SO_4^{2-}/SGH-TiO_2–50–80–1 > SO_4^{2-}/SGH-TiO_2–50–180–1 > SO_4^{2-}/A-TiO_2 ≫ SO_4^{2-}/A-TiO_2 (500 °C). In general, the pore volume of the samples is related to their crystallite size. The pore volume is increased as the anatase crystallite size in the samples becomes finer and more uniform.

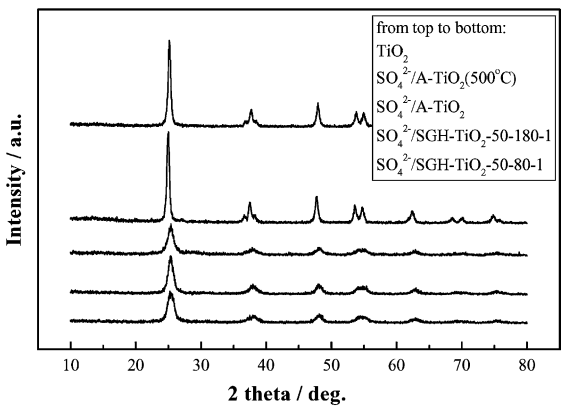

Fig. 5. XRD patterns of various sulfated titania catalysts.

According to the results of chemical analysis, the sulfur content of SO_4^{2-}/SGH-TiO_2–50–80–1 was slightly higher than that of SO_4^{2-}/SGH-TiO_2–50–180–1 and SO_4^{2-}/A-TiO_2. The sulfur content of SO_4^{2-}/A-TiO_2 (500 °C) was much lower than that of all the other catalysts due to the limited initial adsorption of sulfate on the precrystallized anatase precursor with a low surface area.

The surface acidity of the catalysts was measured by NH_3-TPD method. The NH_3-TPD profiles of the sulfated catalysts were shown in Fig. 6. There was only one asymmetric broad peak on the profiles, and no evident peak temperature could be read out from the profiles. The maxima of the NH_3 adsorption peaks were approximately in the range of 350–450 °C, indicating that the catalysts were abundant in medium-strong acid sites. The total amount of acid sites of the catalysts followed the order of SO_4^{2-}/SGH-TiO_2–50–80–1 (0.79 mmol/g) > SO_4^{2-}/SGH-TiO_2–50–180–1 (0.72 mmol/g) > SO_4^{2-}/A-TiO_2 (0.66 mmol/g) > SO_4^{2-}/A-TiO_2 (500 °C) (0.45 mmol/g), which was parallel to the order of their surface area.

3.3. Activity testing

The catalytic behavior of the sulfated titania catalysts towards acid-catalyzed reactions requiring acid

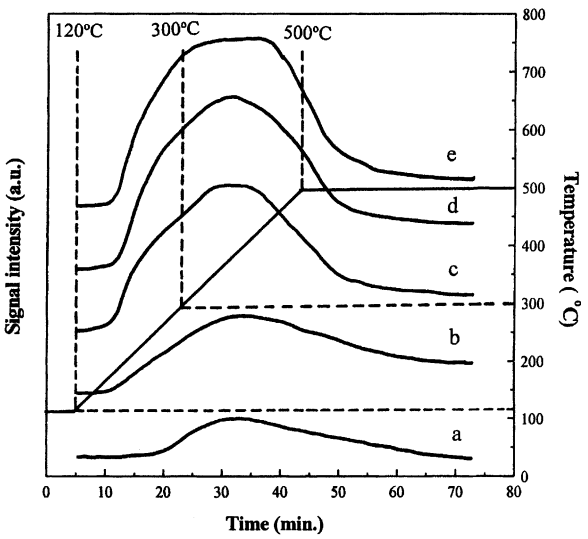

Fig. 6. NH_3-TPD profiles of: (a) A-TiO_2 (500 °C); (b) SO_4^{2-}/A-TiO_2 (500 °C); (c) SO_4^{2-}/A-TiO_2; (d) SO_4^{2-}/SGH-TiO_2–50–180–1; (e) SO_4^{2-}/SGH-TiO_2–50–80–1.

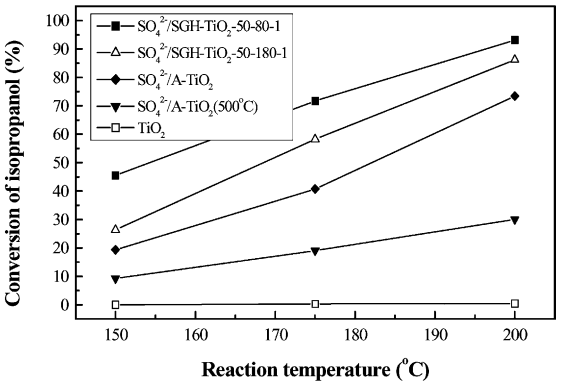

Fig. 7. Conversion of isopropanol as a function of reaction temperature.

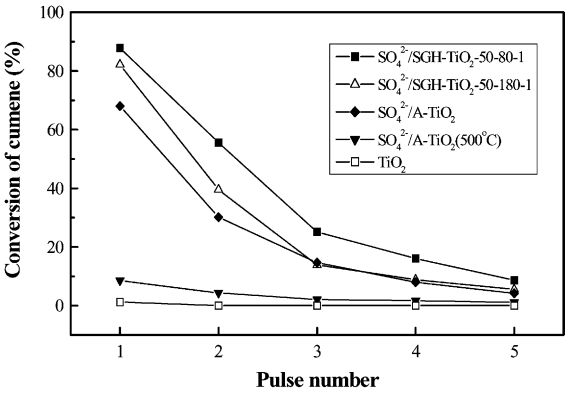

Fig. 8. Conversion of cumene as a function of pulse number at 300 °C.

sites with different acid strengths, such as isopropanol dehydration, cumene cracking and *n*-pentane conversion, has been investigated.

Isopropanol dehydration is known to be catalyzed by weak acid sites. The conversion of isopropanol on various catalysts as a function of reaction temperature was shown in Fig. 7. Non-sulfated TiO_2 was inactive for the reaction under these reaction temperatures, but an obvious enhancement in activity was observed for all the sulfated catalysts. However, there was a marked difference in activity among the catalysts prepared from different titania precursors. At all the three reaction temperatures, the dehydration activity followed the order of SO_4^{2-}/SGH-TiO_2–50–80–1 > SO_4^{2-}/SGH-TiO_2–50–180–1 > SO_4^{2-}/A-TiO_2 > SO_4^{2-}/A-TiO_2 (500 °C), which was the same as that of their total acidity.

Cumene converts to benzene and propene on acid catalysts with medium-strong and strong acid sites. The conversion of cumene dropped rapidly with increasing pulse number because of coking on the sulfated catalysts. The variation of cumene conversion with pulse number on the catalysts at 300 °C was shown in Fig. 8. The initial activity of the catalysts for cumene cracking followed the same order as that for isopropanol dehydration, implying that the SO_4^{2-}/SGH-TiO_2 catalysts have not only greater total acidity but also greater medium-strong and strong acidity.

Table 2
Conversion of *n*-pentane and product distribution on various samples

Catalyst	Product distribution (mol%)							Conversion (%)
	C_1	C_2	C_3	*i*-C_4	*n*-C_4	*i*-C_5	*n*-C_5	
	325 °C							
TiO_2	0	0	0	0	0	0	100	0
SO_4^{2-}/A-TiO_2 (500 °C)	0	0.1	0.1	0	0	0.1	99.7	0.3
SO_4^{2-}/A-TiO_2	0.4	3.4	17.5	0	8.8	0.1	69.8	30.2
SO_4^{2-}/SGH-TiO_2–50–180–1	0.8	6.4	23.2	0.5	5.6	0	63.4	36.5
SO_4^{2-}/SGH-TiO_2–50–80–1	0.9	7.6	29.1	6.4	9.0	0	47.0	53.0
	350 °C							
TiO_2	0	0	0	0	0	0	100	0
SO_4^{2-}/A-TiO_2 (500 °C)	0	0.4	0.7	0.1	0.3	0	98.5	1.5
SO_4^{2-}/A-TiO_2	1.4	11.0	29.4	0.8	4.9	0	52.5	47.5
SO_4^{2-}/SGH-TiO_2–50–180–1	2.1	16.6	38.3	0	3.1	0	39.9	60.1
SO_4^{2-}/SGH-TiO_2–50–80–1	3.2	22.5	47.8	0	4.9	0	21.6	78.4

The catalytic performance of the catalysts in *n*-pentane conversion was similar to that in cumene cracking. The conversion of *n*-pentane also decreased rapidly with increasing pulse number due to coking on the catalysts. The initial conversion of *n*-pentane and the product distribution for different catalysts at 325 and 350 °C were listed in Table 2. The main reaction product was C_3. The selectivity to C_4 was higher than that to C_2 at 325 °C, and au contraire at 350 °C. The sequence of the initial activities of the catalysts in this reaction was similar to that in cumene cracking, which again confirms that SO_4^{2-}/SGH-TiO_2 catalysts have more medium-strong and strong acid sites than SO_4^{2-}/A-TiO_2 and SO_4^{2-}/A-TiO_2 (500 °C) catalysts.

4. Discussion

Experimental results in this work demonstrate that the type of precursor plays an important role in the preparation of sulfated oxide catalysts. The fact that the catalysts prepared from sol–gel hydrothermal derived nanocrystalline anatase TiO_2 have greater surface area and higher catalytic activity than ordinary SO_4^{2-}/TiO_2 catalyst prepared from amorphous titania hydrate tells that to use amorphous oxide as precursor is no more a requisite for the preparation of a good sulfated oxide catalyst. The validity of the generally realized concept that sulfation of crystallized oxide does not produce strong acidity [4] becomes questionable, since both SGH-TiO_2–50–180–1 and SGH-TiO_2–50–80–1 are nanocrystalline anatase TiO_2 with distinct reflections in their XRD patterns. Furthermore, it is also interesting to note that not all nanocrystalline anatase TiO_2 are good precursors. Precrystallized A-TiO_2 (500 °C) with a crystallite size of 50 nm obtained by calcination of amorphous titania belongs to the category of anatase nanocrystals as well, but the sulfated catalyst prepared using A-TiO_2 (500 °C) as a precursor displays low surface area and poor activity. Therefore, it is clear that amorphous or crystalline, crystalline or nanocrystalline are not the watersheds between a good and a poor precursor. Careful measurements of the samples at different preparative stages in the present work suggest that there are other factors controlling the quality of the oxide precursors used for the preparation of sulfated oxide catalysts.

It has been noted that the crystalline grain and specific surface area of the oxide precursor exert a significant influence on the properties of the catalyst. Catalysts obtained by sulfating SGH-TiO_2 with smaller crystalline grain and higher surface area possess greater sulfate content and higher activity, whereas sulfating A-TiO_2 (500 °C) with larger crystalline grain and lower surface area gives unsatisfactory results although both precursors are nanocrystalline anatase TiO_2. Since sulfation of the oxide is carried out by SO_4^{2-} adsorption onto the precursor, a smaller crystalline grain and a higher surface area of the precursor enhance the adsorption and, hence, increase the sulfate content of the final catalyst, even if a part of the sulfate is lost during thermal activation of the catalyst. On the other hand, a larger amount of sulfate adsorbed in the precursor inhibits the sintering of the oxide more efficiently upon calcination [4]. These two reasons may explain the positive effect of the small crystalline grain and high specific surface area of the SGH-TiO_2 precursors on the properties of the final sulfated oxide catalysts.

Nevertheless, the initial surface area is not the sole criterion for an oxide precursor, because the surface area and activity of SO_4^{2-}/A-TiO_2 catalyst prepared from amorphous A-TiO_2 with a BET surface area as high as 367 m^2/g are appreciably lower than those of SO_4^{2-}/SGH-TiO_2 catalysts. Such an apparent abnormality may be explained on the basis of thermostability. After sulfation, the titania precursors must be calcined at a high temperature (>500 °C) to produce strong acidity. In our previous work, it has been observed that the transition of amorphous TiO_2 to crystalline anatase TiO_2 takes place at 350 and 500 °C for pure TiO_2 and sulfated TiO_2, respectively [13]. The phase transition is accompanied by a significant reduction in surface area as shown in Fig. 2. Meanwhile, the nanocrystals of anatase TiO_2 in sulfated SGH-TiO_2 samples are more thermally stable. Upon calcination, there is no phase transition and the presence of SO_4^{2-} species stabilizes the surface area, so the final SO_4^{2-}/SGH-TiO_2 catalysts retain higher surface areas and higher catalytic activities.

The structure of the surface sulfate complex and the nature (Lewis or Bronsted type) of the strong acid sites on sulfated oxide catalysts are still a subject of debate, because technological advances to date are inadequate for a complete characterization

of these catalysts. However, information in the literature [12,30–32] show that the texture of sulfated zirconia catalysts prepared from amorphous, aerogel and precrystallized zirconia differs from each other, but the feature of the active sites on these catalysts is much the same. This is probably also true for sulfated titania catalysts prepared from different precursors according to the results of this work. From the XRD, NH_3-TPD and activity measurements there is no evident indication that the nature of the surface sulfate species has been altered due to the change of precursors. The acidity and the catalytic activities of the catalysts toward various acid-catalyzed reactions correlate fairly well with their sulfur content and specific surface area, implying that the variation in texture of the catalysts rather than in structure or nature of the active sites accounts for the difference in the catalysts.

Acknowledgements

This work was supported by the Major State Basic Research Development Program (Grant no. 2000077507) and the Foundation for University Key Teacher by the Ministry of Education.

References

[1] K. Arata, Adv. Catal. 37 (1990) 165.
[2] B.H. Davis, R.A. Keogh, R. Srinivasan, Catal. Today 20 (1994) 219.
[3] A. Corma, Chem. Rev. 95 (1995) 559.
[4] X. Song, A. Sayari, Catal. Rev. Sci. Eng. 38 (1996) 329.
[5] G.D. Yadav, J.J. Nair, Micropor. Mesopor. Mater. 33 (1999) 1.
[6] K. Tanabe, H. Hattori, T. Yamaguchi, Crit. Rev. Surf. Chem. 1 (1990) 1.
[7] F.R. Chen, G. Coudurier, J.F. Joly, J.C. Vedrine, J. Catal. 143 (1993) 616.
[8] C. Guo, S. Yao, J. Cao, Z. Qian, Appl. Catal. A 107 (1994) 229.
[9] R.A. Comelli, C.R. Vera, J.M. Parera, J. Catal. 151 (1995) 96.
[10] C. Morterra, G. Cerrato, F. Pinna, M. Signoretto, J. Catal. 157 (1995) 109.
[11] T. Riemer, D. Spielbauer, M. Hunger, G.A.H. Mekhemer, H. Knozinger, Chem. Commun. (1994) 1181.
[12] Y.Y. Huang, B.Y. Zhao, Y.C. Xie, Appl. Catal. A 172 (1998) 327.
[13] Z. Gao, J.M. Chen, Chem. J. Chin. Univ. 15 (1994) 873.
[14] Z. Gao, J.M. Chen, W.M. Hua, Y. Tang, Stud. Surf. Sci. Catal. 90 (1994) 507.
[15] A.K. Dalai, R. Sethuraman, S.P.R. Katikaneni, R.O. Idem, Ind. Eng. Chem. Res. 37 (1998) 3869.
[16] A. Corma, A. Martinez, C. Martinez, Appl. Catal. A 144 (1996) 249.
[17] A. Hess, E. Kemnitz, Appl. Catal. A 149 (1997) 373.
[18] S.K. Samantaray, T. Mishra, K.M. Parida, J. Mol. Catal. A 156 (2000) 267.
[19] Y.D. Xia, W.M. Hua, Z. Gao, Catal. Lett. 55 (1998) 101.
[20] W.M. Hua, Y.D. Xia, Y.H. Yue, Z. Gao, J. Catal. 196 (2000) 104.
[21] G.Z. Lu, Appl. Catal. A 133 (1995) 11.
[22] J. Lin, Chin. J. Org. Chem. 20 (2000) 805.
[23] J. Lin, H.T. Liu, R.Q. Zhao, Chin. J. Inorg. Chem. 16 (2000) 829.
[24] X.Z. Fu, W.A. Zeltner, Q. Yang, M.A. Anderson, J. Catal. 168 (1997) 482.
[25] Z. Ma, W.M. Hua, Y. Tang, Z. Gao, Chin. J. Chem. 18 (2000) 341.
[26] X.Z. Fu, Z.X. Ding, W.Y. Su, D.Z. Li, Chin. J. Catal. 20 (1999) 321.
[27] W.Y. Su, X.Z. Fu, K.M. Wei, Acta Physico-Chimica Sinica 17 (2001) 28.
[28] S.M. Jung, P. Grange, Catal. Today 59 (2000) 305.
[29] C.C. Wang, J.Y. Ying, Chem. Mater. 11 (1999) 3113.
[30] C. Morterra, G. Cerrato, V. Bolio, Catal. Today 17 (1993) 505.
[31] C.X. Miao, Z. Gao, Mater. Chem. Phys. 50 (1997) 15.
[32] A.F. Bedilo, K.J. Klalunde, J. Catal. 176 (1998) 448.